

Interstitial atoms in tungsten: Interaction with free surface and *in situ* determination of formation energy

I. M. Neklyudov, E. V. Sadanov, G. D. Tolstolutskaia, V. A. Ksenofontov, T. I. Mazilova, and I. M. Mikhailovskij*

National Scientific Center, Kharkov Institute for Physics and Technology, Akademicheskaja, 1, Kharkov 61108, Ukraine

(Received 26 June 2008; published 19 September 2008)

The energy of formation of self-interstitial atoms has been experimentally determined using an energy analysis of low-temperature field evaporation of tungsten in a field-ion microscope. An experimental approach, based on the strong dependence of the threshold field for evaporation on the total energy of the surface atoms, is used. It was found that the excited atomic states can be produced by the release of the formation energy of self-interstitial atoms emerging at the surface. The experimental results are discussed in the framework of the image-hump model of field evaporation and compared with theoretical data on the energy of formation of interstitial atoms.

DOI: [10.1103/PhysRevB.78.115418](https://doi.org/10.1103/PhysRevB.78.115418)

PACS number(s): 61.72.Bb, 66.30.Fq

Point defects can be created in solids under different types of treatment such as high-temperature annealing, plastic deformation, and irradiation. In metals the vacancies have a formation energy lower than that of self-interstitial atoms (SIAs) and are consequently the defects that ensure the atomic diffusion at thermal equilibrium. The situation is basically different for materials irradiated with energetic particles for which the concentration of both SIAs and vacancies may be orders of magnitude higher than the equilibrium ones. Self-interstitials easily move because they have migration energies lower than that of vacancies and are one of the factors driving microstructure in metals. Among the extrinsic atomic defects produced under irradiation, the SIAs are significant due to the large lattice distortion they cause.^{1,2} The properties of SIAs are of particular interest since their production, migration, and annihilation control the yield strength, ductility, and radiation-induced swelling of metallic alloys in nuclear materials. In a radiation environment, SIAs are the dominant defect in nonequilibrium states of metals. There have been many theoretical studies on the radiation damage of body-centered-cubic (bcc) transition metals as nuclear fusion reactor materials. Recent computer simulations showed that, in bcc metals, a SIA adopts one of several possible configurations, each having its characteristic formation energy.¹⁻⁴ The most important SIA configuration is the $\langle 111 \rangle$ crowdion/dumbbell that has the lowest energy of formation. Knowledge of the energetics of self-interstitials is a significant prerequisite for studying the mechanism driving microstructural evolution of materials under irradiation. For all the transition metals, the energy of SIA formation is several times lower than the energy of formation of vacancies.^{5,6} As a result, SIAs do not spontaneously form in bcc metals at high temperatures. The energy of vacancy formation can be found out experimentally and theoretically, whereas the SIA formation energy is less accessible to direct determination due to the large lattice distortion. Determination of the SIA formation energy is decisive as an initial point to understand the lattice defect behavior and the evolution of microstructure of irradiated nuclear fusion reactor materials.⁵

In the research that is reported here, we determined *in situ* the SIA formation energy E_i^f in bcc-W using the field-ion microscopy (FIM) based method. Tungsten was chosen for

several reasons. First, W is a typical example of the bcc transition metals, which provide important structural materials for fusion reactors^{5,6} and nanotechnology.⁷ Second, the most reliable experimental data on field-ion characteristics⁸ and radiation damage^{9,10} were obtained before for W. Third, tungsten was chosen also because theoretical calculations of self-interstitial properties for W have been reported recently.¹⁻⁵ These calculations provide a cross-check on the accuracy of the data of the current investigation.

The FIM method for measuring E_i^f , such as the known method for determining the binding energy of atoms Λ ,^{11,12} is based on low-temperature field evaporation, which is characterized by a strong dependence of the threshold field for evaporation on the total energy of the surface atoms. Field evaporation, the removal of surface atoms by applied high electric field at low temperatures where field-free thermal evaporation is ineffective, is of significance in atom-probe field-ion microscopy and related techniques, and is of interest to nanotechnology and nanoscience.^{8,13} Theories of low-temperature field evaporation of metals are now fairly well developed. As is known, the Müller-Schottky (“image-hump”) analytic model corrected for postionization, in spite of its limitations discussed in Refs. 8, 12, and 13, has been quite successful in predicting the experimentally determined evaporation field at low temperatures and charge distribution for field-evaporated atoms. We used this model for the estimation of the kinetic energy of individual atoms in the highly excited state that arose due to the release of the formation energy of interstitial atoms emerging at the free surface.

The *in situ* experiments were carried out using a two-chamber field-ion microscope with samples cooled to 21 K within an accuracy of $-0.4/+4$ K and a residual gas pressure of 10^{-7} Pa.¹⁴ The FIM was equipped with a source of accelerated monoenergetic helium atoms. Helium at a pressure of 10^{-3} – 10^{-2} Pa was used as an imaging gas. Needle-shaped samples (tips) with radius of curvature of 20–100 nm were prepared from a tungsten wire of 99.98% purity by electrochemical etching. After mounting in the microscope, the samples were subjected to low-temperature field evaporation until an atomically flat surface was formed. The tips were bombarded with neutral helium atoms with an energy of 2–7 keV and a flux of $(5-20) \times 10^{15}$ atoms/(m² s). The

bombardment was accomplished in the direction perpendicular to the sample axis. Since the neutral atoms do not deflect in the electric field of the samples, the possibility exists of examining the elementary events of surface erosion in high electric fields. During the bombardment and for 10–60 s after completion of irradiation, the appearance of emission centers was observed at the surface areas not subjected to the bombardment (shadow region).

During the evaporation, the electric field was constant at a level of $(5.75 \pm 0.10) \times 10^{10}$ V/m. After surface cleaning by evaporation, the electric field was reduced to the level of $(4-5) \times 10^{10}$ V/m. At such fields an ionization barrier is created near the surface,¹² preventing the residual gas atoms, which are characterized by relatively low ionization potentials, from reaching the investigated part of the sample. Thus, the ultrahigh-vacuum conditions and the presence of a field-ionization barrier prevented the residual gas atoms from striking the surface under study. The migration of residual gases adsorbed on the surface of the shank of the sample, which was not shielded by the ionization barrier, was insignificant at 21 K and did not lead to contamination of the investigated part of the sample.

Figure 1 shows FIM images of the surface of the tungsten sample oriented along the $[141]$ direction (a) before and (b) after bombardment with fluence of 4.1×10^{16} atoms/m² at a field strength of 4.1×10^{10} V/m. The bombardment by helium atoms was carried out in the $[3\bar{1}\bar{2}]$ direction, nearly perpendicular to the tip axis. The field strength was calculated from the ratio of the operating voltage to the threshold voltage for the evaporation of tungsten at 21 K, which corresponds to a field of 5.8×10^{10} V/m. SIAs that reached the shadow surface area and were converted into single adatoms were detected as additional centers of a high emission contrast [marked by arrows in Fig. 1(b)]. The formation of adatoms was observed directly in the field-ion microscope both in the course of irradiation and for about 1 min after switching off the source of accelerated helium atoms. This provides evidence for the nondynamic character of the surface damage process. In the temperature range studied, only the interstitial tungsten atoms are mobile. One can thus conclude that the formation of adatoms after switching off the source of accelerated atoms is the result of the diffusion of radiation-induced interstitial atoms to the surface. Analysis of the radiation-induced changes in the surface morphology suggests that, apart from the single adatoms, the dimer configurations of adatoms can be produced. An example of the pair of adatoms on the (231) facet is pointed out by the arrowhead in Fig. 1(b).

Our studies showed that the number of atoms that reached the shadow surface area and were detected after the bombardment was strongly dependent on the field applied during the bombardment. As the field was raised from 4.4×10^{10} to 4.6×10^{10} V/m, the number of atoms detected decreased essentially to zero. At fields below 4.3×10^{10} V/m, the flux of interstitial atoms J_i , which were detected, was independent of the field and was approximately equal to the flux of atoms, of radiation origin, reaching the surface in the absence of the field J_0 (see Fig. 2). To remove the atoms that reached the surface and became adsorbed on the (110) facets, we need

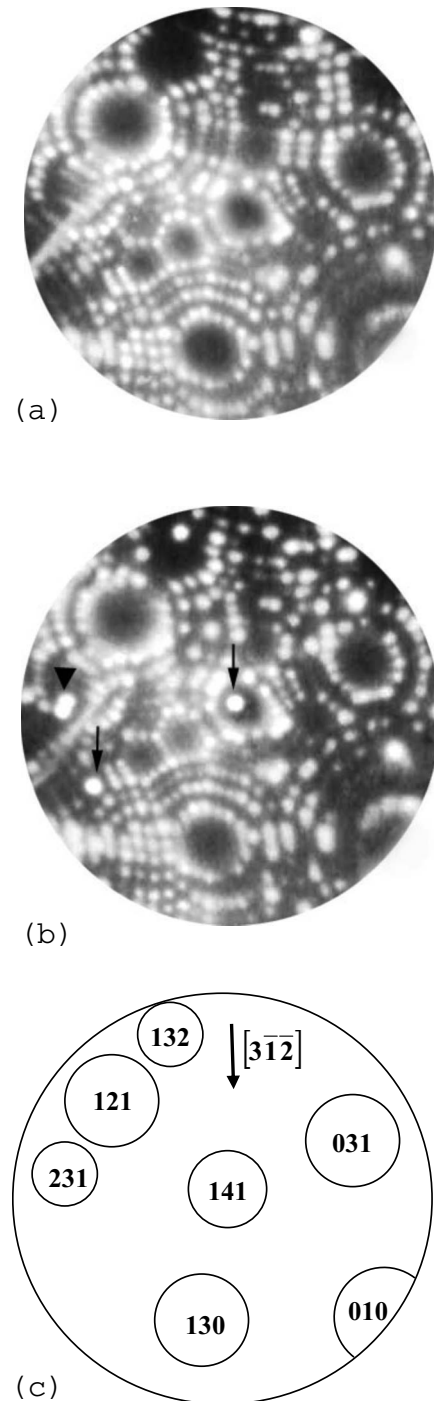


FIG. 1. FIM images of the surface of tungsten needle-shaped monocrystal (a) before and (b) after the bombardment with neutral helium atoms with an energy of 6.5 keV and a fluence of 4×10^{16} atoms/m², and (c) corresponding stereographic projection. Arrows indicate (b) the surface point defects and (c) the bombardment direction.

substantially stronger electric fields: $F_d = (5.1 \pm 0.4) \times 10^{10}$ V/m. Atoms at the (110) surface steps [see Fig. 1(b)] evaporate at field $(5.75 \pm 0.10) \times 10^{10}$ V/m. For atoms on the (141) facets, $F_d = (5.80 \pm 0.10) \times 10^{10}$ V/m. The lifetime τ of surface atoms at these fields is about 10 s. The difference between desorption fields is evidence that the energy of

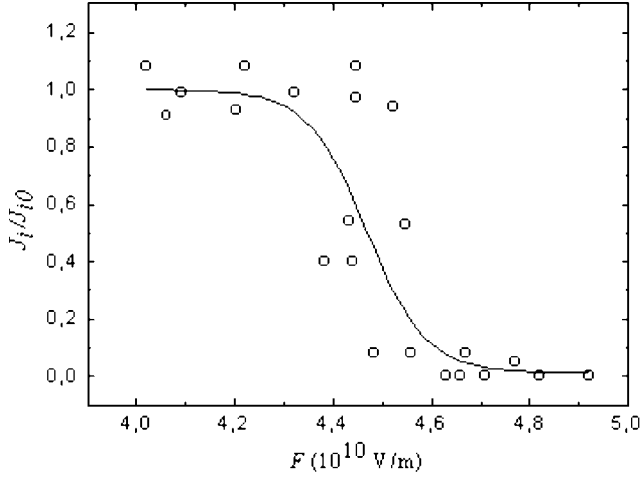


FIG. 2. Dependence of the reduced flux of interstitial atoms detected at the shadow surface region after the bombardment with 6.5 keV helium atoms on the field strength.

formation of a SIA that is released strongly influences the field-evaporation process. The difference between the threshold evaporation fields for the excited state F_{es} and ground state F_d of adatoms was observed not only during the bombardment but also after switching off the ion source. This additionally points to the fact that low-temperature field evaporation is promoted by the energy of SIAs with high diffusive mobility that reached the surface. Strictly, direct comparisons should not be made between fields F_{es} and F_d since these values relate to drastically different rates of field evaporation. The threshold field F_d for the ground state corresponds to the field-evaporation rate $K_{e0} = \tau^{-1}$, equal to about 0.1 atoms/s, while the field-evaporation rate in the excited state is determined by the lifetime of surface atoms of the order of the period of an atomic vibration τ_0 ($\sim 10^{-13}$ s).

For strongly bound surface atoms (evaporation energy $\gg k_B T$), the provision of a limited amount of kinetic energy promotes field evaporation without changing the fundamental mechanisms involved.¹² The revealed difference between evaporation fields for the excited and ground states of adatoms can be described quantitatively on the basis of the image-hump model of field evaporation^{12,13} in which ionization of atoms precedes escape. The potential energy of a SIA ($x < 0$), a surface atom ($x \approx 0$), and an ion near a metal surface ($x > 0$) in a high electric field for this model is shown in Fig. 3, where x is the distance from the effective electron surface (or image plane) of the metal. In this model, the potential in the intermediate distance ($x \approx 0$), shown in the diagram by a broken curve, is not clearly defined. The binding energy of the neutral surface atom was found to be identical to the cohesive energy Λ of metal and independent of the applied field F .¹¹ The activation energy $Q_n(F)$ necessary for an initially neutral atom to escape over the Schottky hump as an n -fold ion is given by

$$Q_n(F) = \Lambda + \sum_n I_n - n\varphi - \sqrt{\frac{n^3 e^3 F}{4\pi\epsilon_0}}, \quad (1)$$

where I_n is the n th ionization energy of the atom, φ is the work function of the metal, and ϵ_0 is the electric constant.

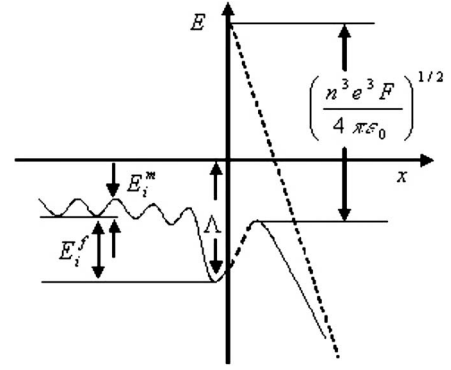


FIG. 3. Potential energy diagram for field evaporation of a self-interstitial atom showing the position of the Schottky hump in the presence of the external electric field. The distance x is reckoned from an effective electron surface.

The evaporation field at absolute zero is correspondent to so-called zero- Q evaporation field F_e —the field at which Q_n would become zero. Determination of F_e is difficult for some reasons. First, there are several possible mechanisms for the escape stage that would predict different F_e values. Second, the fields are determined for different charge states n and the field F_e is identified as the lowest of these. Recently the zero- Q evaporation field for tungsten $F_e = 6.0 \times 10^{10}$ V/m was obtained and it was shown that it can be used for a legitimate comparison of experiment with theory of field evaporation.⁸ In the case of $Q_n \approx 0$, the time required to overcome an energy barrier τ_0 is essentially equal to the inverse of the vibrational frequency of the surface atom.

The SIA formation energy E_i^f is determined as the difference between the potential energy of a relaxed crystallite containing the SIA and the potential energy of a perfect crystallite containing the same number of atoms. The energy E_i^f is corresponded to embedding an extra atom in the crystal lattice followed by the minimization of the potential energy of all the atoms. It is usually reckoned from the energy level of a surface atom bound to a surface kinked step. As can be seen from the energy diagram in Fig. 3, the potential energy of a near-surface self-interstitial atom lies above the ground state of a surface atom in a defect-free lattice. As a result, the image-force barrier is overcome at comparatively low values of the field strength. When a self-interstitial atom migrates toward the surface, its excess energy E_i^f decreases by an amount equal to the work performed by the image forces to the level E_{is}^f in the last near-surface interstitial position. This work is of the order of energy of the migration barrier E_i^m . Since usually $E_i^m \ll E_i^f$, we can assume that the energy released by the interstitial atoms emerging at the surface is close to the total energy of formation ($E_i^f \approx E_{is}^f$). After surmounting the last surface barrier, the interstitial atom is in a near-surface adsorption well with nearly the same energy E_{is}^f as before the transition since it has not managed to transfer this excess energy to the lattice. In other words, the atom is in a highly excited state in the adsorption well. A certain time later, the atom goes to the adsorption ground state in the course of a relaxation process. Consequently, an electric field can evaporate adsorbed atoms from either the ground state or the highly excited state. If the field is high enough, the for-

mation of adatoms as a result of the diffusion of SIAs to the surface and field evaporation may occur simultaneously (within the time of one to a few atomic vibrations τ_0). Thus, the fact that the evaporation fields for the atoms in the nascent adsorption state F_{es} and in the relaxed state F_d are different is evidence that the atoms in the adsorption state bear an excess energy. The lifetime of the excited-state atom is comparable with that of zero- Q evaporation.

In this way the SIA formation energy E_i^f will be available in promoting field evaporation and, in light of this, Λ in Eq. (1) must be replaced by $(\Lambda - E_i^f)$. The evaporation process can be regarded as consisting of two steps: the first being the desorption of the neutral surface atom in an anomaly excited state, and the second being the field ionization of this species and overcoming the Schottky hump. Since the evaporating field depends strongly on the total energy of the evaporated atom, the unknown quantity E_{is}^f , nearly equal to E_i^f , can be determined from the difference between the evaporating fields in these two states. Strictly speaking, the quantities Λ , E_{is}^f , and φ depend on crystallographic orientation and curvature of the surface region under study. In order to reduce the error, we would thus like to determine E_i^f from the difference between the zero- Q evaporation field F_e and the threshold evaporation field for the excited state F_{es} with the same lifetime of pre-evaporation states:

$$E_i^f = \sqrt{\frac{n^3 e^3}{4\pi\epsilon_0}} (F_e^{1/2} - F_{es}^{1/2}) + \Delta E_i, \quad (2)$$

where ΔE_i is the correction term equal to the kinetic energy transferred to the lattice by the SIA emerging at the free surface. Early molecular-dynamics simulations¹⁵ performed using the Johnson pair potential for tungsten showed that $\Delta E_i = 0.26E_i^f$ for self-interstitial atoms emerging at the (141) facet (see Fig. 1). At low temperatures, tungsten is evaporated for the most part as threefold ionized atoms.^{12,13} Taking

into account that $E_i^f \approx E_{is}^f$ and substituting the values $F_e = 6.0 \times 10^{10}$ V/m, $F_{es} = (4.45 \pm 0.10) \times 10^{10}$ V/m, and $n=3$, we find the SIA formation energy to be $E_i^f = 9.06 \pm 0.63$ eV.

This value is in agreement with the available theoretical predictions for the SIA formation energy in bcc tungsten, which lie between 8.92 eV for stable and 9.55 eV for metastable configurations.^{1,2} Since differences are within statistical uncertainties, the comparison of the experimental and theoretical E_i^f values does not provide strong support for one theoretical model over another. Moreover, this agreement does not rule out the possibility of systematic errors in the developed experimental method but it does show that possible errors cannot be overly significant. In particular, the agreement supports the assumption that the work performed by the image forces in moving an interstitial atom from the interior to the subsurface atomic layer is small.

To summarize, we have shown that the energy of formation of self-interstitial atoms can be measured directly from an energy analysis of low-temperature field evaporation using a field-ion microscope. It appears that the excited surface atomic states can be produced by the release of the formation energy of self-interstitial atoms emerging at the surface. This effect has manifested itself in the field-ion microscope by the difference between the threshold fields of evaporation in the excited and ground states. The FIM based method was applied to tungsten specimens saturated with the interstitial atoms *in situ* produced during the bombardment with accelerated helium atoms. The energy of formation of interstitial atoms in tungsten determined by the FIM based method is found to be in satisfactory agreement with the recent theoretical data.

The authors would like to thank Richard G. Forbes for stimulating comments. This work was supported by the Program of Basic Researches on Nanotechnology of the National Academy of Sciences of the Ukraine and the NATO International Program No. SA (PST.CLG.976376) 5437.

*mikhailovskij@kipt.kharkov.ua

¹P. M. Derlet, D. Nguyen-Manh, and S. L. Dudarev, Phys. Rev. B **76**, 054107 (2007).

²D. Nguyen-Manh, A. P. Horsfield, and S. L. Dudarev, Phys. Rev. B **73**, 020101(R) (2006).

³C. S. Becquart and C. Domain, Nucl. Instrum. Methods Phys. Res. B **255**, 23 (2007).

⁴Y. Satoh, H. Matsui, and T. Hamaoka, Phys. Rev. B **77**, 094135 (2008).

⁵D. Nguyen-Manh and S. L. Dudarev, Mater. Sci. Eng., A **423**, 74 (2006).

⁶M. Mrovec, R. Gröger, A. G. Bailey, D. Nguyen-Manh, C. Elsässer, and V. Vitek, Phys. Rev. B **75**, 104119 (2007).

⁷S. Chattopadhyay, L.-C. Chen, and K.-H. Chen, Crit. Rev. Solid State Mater. Sci. **31**, 15 (2006).

⁸D. N. Zurlev and R. G. Forbes, J. Phys. D **36**, L74 (2003).

⁹Y. Zhong, K. Nordlund, M. Ghaly, and R. S. Averback, Phys. Rev. B **58**, 2361 (1998).

¹⁰T. I. Mazilova and I. M. Mikhailovskij, Surf. Interface Anal. **36**, 510 (2004).

¹¹J. Liu, C. Wu, and T. T. Tsong, Phys. Rev. B **43**, 11595 (1991).

¹²M. K. Miller, A. Cerezo, M. G. Heatherington, and G. D. W. Smith, *Atom Probe Field Ion Microscopy* (Clarendon, Oxford, England, 1996).

¹³T. T. Tsong, *Atom-Probe Field Ion Microscopy* (Cambridge University Press, Cambridge, England, 1990).

¹⁴I. M. Mikhailovskij, G. Smith, N. Wanderka, and T. I. Mazilova, Ultramicroscopy **95**, 157 (2003).

¹⁵T. I. Mazilova, Ph.D. thesis, Kharkov Institute of Physics and Technology, 1996.